Solar Probe: A Mission to the Sun and the Inner Core of the Heliosphere

G. Gloeckler[1], W. C. Feldman[2], S. R. Habbal[3], R. L. McNutt[4], J. E. Randolph[5], A. Title[6] and B. T. Tsurutani[5]

[1]University of Maryland, College Park, Maryland, 20742

[2]Los Alamos National Laboratory, Los Alamos, New Mexico, 87545

[3]Harvard-Smithsonian Center for Astrophysics, Cambridge, Massachusetts, 02138

[4]Applied Physics Laboratory, Johns Hopkins University, Laurel, Maryland, 20723

[5]Jet Propulsion Laboratory, Pasadena, California, 91109

[6]Lockheed Research, Palo Alto, California, 94304

Abstract Solar Probe, the first mission to the Sun, is a mission of exploration, discovery and comprehension. Solar Probe will address the basic question of solar wind origin by flying through the acceleration region where the wind is born, and will determine solar surface topology over the poles. Despite the extraordinary observations with Ulysses and SOHO, only Solar Probe measurements made close to the Sun and over its poles can provide closure to these fundamental problems. Solar Probe, scheduled for launch in February 2007 will arrive at the Sun in 2010 flying along a polar trajectory perpendicular to the Sun-earth line during perihelion passage 3 solar radii above the Sun's surface. The second closest approach will be near solar minimum in 2015. Both imaging and in-situ miniaturized instruments will provide the first three-dimensional view of the corona, high spatial and temporal observations of the magnetic fields and helioseismic measurements of the solar polar regions, as well as local sampling of plasmas and fields at all latitudes. Following a brief review of our current knowledge of the solar wind and processes on the solar surface, we describe the baseline Solar Probe mission, its prime scientific objectives and its strawman instrument payload.

1. INTRODUCTION

One of the last unexplored regions of the solar system is the innermost portion of the heliosphere, the region inside the orbit of Mercury, the region that reaches to within a few solar radii (R_S) from the Sun's surface. We have flown by many planets. Galileo is now orbiting Jupiter and Cassini is on its way to circle Saturn. With Ulysses we are exploring

the high latitude heliosphere and the Voyagers are soon expected to reach and report on the distant boundary of the solar system. From its 1 AU orbit SOHO is imaging the Sun far better than ever before and the 1 AU solar wind and solar energetic particles are measured in greater detail and with greater precision than ever before with WIND and ACE. Yet we have never encountered the Sun. The inner heliosphere, the polar photosphere and the solar corona remain essentially unknown. We do not understand how the Sun creates its pervasive solar wind which affects the earth, all the planets and determines the size of the heliosphere and interacts with the local interstellar cloud surrounding the solar system. We do not understand what processes heat the solar corona and how the energy responsible for this heating flows through the solar atmosphere.

It is now technically possible to send a well-instrument and affordable spacecraft close to the Sun's surface to explore for the first time this last frontier, the inner heliosphere from a few to ~100 R_S. Solar Probe is this mission.

Solar Probe is a mission of exploration, of discovery and of comprehension. Flying from pole to pole through the solar atmosphere, as close as 3 R_S above the solar surface, Solar Probe will perform the first close-up exploration of the Sun, the only star accessible to humankind. This pioneering mission will sample directly the solar wind in the acceleration region and will take high resolution images of the solar atmosphere, especially of the polar regions of the Sun. This missing "ground " truth picture will link the enormous wealth of existing solar and coronal observations to the actual physical state and dynamics of the solar corona. Solar probe will determine the origin and acceleration of the solar wind which engulfs the entire solar system, modulates the penetrating cosmic rays from the galaxy into the solar system and onto earth, and controls interplanetary space from the Sun to the local interstellar medium far beyond the outermost planets. Solar Probe is the third of three missions in NASAs Outer Solar System/Solar Probe Program.

2. CURRENT KNOWLEDGE OF THE INITIAL AND TERMINAL SOLAR WIND AND OF THE SOLAR SURFACE

Recent measurements with state-of-the-art instruments on Ulysses, SOHO, Wind and ACE have advanced our current understanding of the initial and terminal solar wind and of the characteristics of the solar surface. We will now briefly review some of the new results and discuss unresolved questions concerning solar wind origin and acceleration.

Fast and Slow Solar Wind. Ulysses observations have shown quite clearly that the solar wind comes in two distinct states. The slow wind with typical speed of about 400 km/s, observed for many years, is most commonly found near the ecliptic plane. The fast

wind, with speed around 800 km/s flows everywhere in the greater than ~30° high latitude regions of the heliosphere, as revealed dramatically with Ulysses (see Fig. 1).

The Fast Wind is Steady and Simple and Dominates the High Latitudes Heliosphere. Ulysses with its near polar 1.4 by 5.4 AU orbit has shown that around solar minimum the fast wind dominates the heliosphere. Fig. 1 also shows that the high speed stream as steady. Composition measurements with the SWICS instrument on Ulysses also reveal that the fast wind is relatively simple. The charge state distribution is characterized by a single, low freezing-in coronal temperature for each element (Geiss et al., 1995) as shown in Fig. 2. The elemental composition of the solar wind is least biased in the fast wind and resembles most closely the photospheric composition, and the overabundance of low FIP (first ionization potential) elements is at most weak as shown in Fig. 3 (Geiss et al., 1995). The isotopic ratio of $^3He/^4He$ has its lowest and least variable values in the fast wind (Gloeckler and Geiss, 1998).

The Slow Wind is Variable and Complicated, and is Confined to the near Ecliptic Heliosphere. In contract to the fast wind, the slow wind, found mostly near the ecliptic plane, is highly variable in speed (see Fig. 1) and more complicated in its other characteristics. The charge state distribution can no longer be characterized by a single freezing in temperature as shown in Fig. 4 (von Steiger et al., 1997). The FIP effect is far more pronounced (see Fig. 3) and the $^3He/^4He$ ratio is both higher and more variable in the slow wind compared to the fast wind (Gloeckler and Geiss, 1998).

Boundary Between the Fast and Slow Wind is Sharp. A systematic study of the solar wind composition across the boundary between the slow and fast wind indicates that the boundary between these two winds is sharp, with step function transition in the freezing-in temperature (as measured by the O^{6+}/O^{7+} ratio) and FIP strength (measured by the Mg/O ratio). These results (Geiss et al., 1995), shown in Fig. 5, indicate that this sharp boundary seen in the speed change at several AU extends down to the lower corona, where the charge states freeze-in and the chromosphere near the solar surface, where the composition is established.

Source of the Fast Wind is an Open Question. The Ulysses results indicate that the fast wind originates in the cool, open field regions of the polar coronal holes and reaches the lower latitudes by superradial expansion. It is not clear, however, from the remote Ulysses observation whether the fast wind comes from the newly discovered solar plumes or the interplume regions of the coronal holes. Recently Habbal et al. (1997) have proposed, on the basis of radio occultation measurements, that the fast wind may also originate outside coronal holes, in the quiet but not active regions of the sun. The slow

wind appears to come from regions outside the coronal hole. However, to isolate the various regions in the equatorial belt will not be possible using remote observations of the terminal wind because of the strong intermixing of the various flows by the time they reach ~ 1 AU (Gloeckler et al, 1998).

Characteristics of the Initial Solar Wind. SOHO observations have revealed some surprising properties of the initial solar wind, the state of the wind in the first few solar radii above the solar surface. The SOHO/UVCS results based on Doppler-dimming observations of the corona below 10 R_S (Kohl et al., 1997; 1998; Li et al., 1998) are summarized in Fig. 6. It is evident that the coronal hole wind reaches its terminal speed of 800 km/s at 10 R_S and that at 4 R_S the solar wind is still being accelerated. The temperature of heavy ions is much larger than that of protons in the coronal hole as well as the equatorial regions. The proton temperature at 3 R_S in the coronal hole is a factor of two to three higher than the electron temperature inferred from charge state measurements in the terminal wind. The proton temperature in the equatorial regions, however, seems to be lower than the inferred electron temperature.

Properties of the Equatorial Photosphere. SOHO measurements, especially from the MDI experiment, have revealed some remarkable features of the equatorial photosphere and have provided some indications of conditions at the polar photosphere which cannot be viewed effectively by SOHO (or any spacecraft confined to the ecliptic plane). Some of the key findings are: (1) the magnetic flux in equatorial regions is replaced very rapidly, about every 40 hours; (2) measurements of surface and subsurface motion indicate meridional flows that are a factor of more than two higher than previously estimated; (3) the rotation rate at higher latitudes is about 10% to 20% lower than was expected; (4) there is some evidence for a polar vortex; (5) there are indications that small and large scale magnetic fields on the sun are rooted at different depths in the convection zone; and (6) there is evidence that polar plumes, associated with strong unipolar fields, stable to ~30 R_S and replenished with plasma every few days, may be sources of the fast solar wind.

Unresolved Questions. The recent results summarized above have not resolved many fundamental questions regarding solar wind origin and mechanisms for its acceleration, or of coronal heating mechanisms and flow of energy from the solar surface to the corona. We do not know magnetic field topology and surface and subsurface flow patterns in the polar regions and how they differ from those at lower latitudes. We have no direct information on the nature of wave turbulence and of wave-plasma interactions in the acceleration region. These questions will remain unanswered until in situ measurements in the solar wind acceleration region near the sun are made and high-resolution images of the

polar regions of the Sun are taken. These open questions are the basis for the Solar Probe Mission

3. SOLAR PROBE: THE FIRST CLOSE ENCOUNTER WITH THE SUN

The Solar Probe Science Definition Team (SDT) listed in Table 1 was charged with providing the prime scientific objectives for the Solar Probe mission and a core strawman instruments payloads to address these objectives. The science objectives were further prioritized by the SDT into three categories: (A) irreducible core objectives to be fulfilled with the baseline instruments payload, (B) objectives that would require minimum enhancement to the payload, and (C) objectives that that could be addressed with additions to the core payload. The SDT also identified payload and measurement requirements, including nadir viewing for the plasma and remote sensing instruments viewing the solar surface. The core payload requirements were then used for the baseline spacecraft and mission design.

Prime Scientific Objectives. The three categories of the Solar Probe prime scientific objectives are given below:

Category A Objectives

- Determine the acceleration processes and find the source regions of the fast and slow solar wind at maximum and minimum solar activity
- Locate the source and trace the flow of energy that heats the corona
- Construct the three-dimensional density configuration from pole to pole, and determine the subsurface flow pattern, the structure of the polar magnetic field and its relationship with the overlying corona
- Identify the acceleration mechanisms and locate the source regions of energetic particles, and determine the role of plasma turbulence in the production of solar wind and energetic particles

Category B Objectives

- Investigate dust rings and particulates in the near-sun environment
- Determine the outflow of atoms from the Sun and their relationship to the solar wind
- Establish the relationship between remote sensing, near-earth observations at 1 AU and plasma structures near the Sun

Category C Objectives

- Determine the role of X-ray microflares in the dynamics of the corona
- Probe nuclear processes near the solar surface from measurements of solar gamma-rays and slow neutrons

Science Core Payload. The strawman payload consists of five in-situ and three remote-sensing miniaturized instruments. The measurements required to address the Category A science objectives are listed for each of these instrument in Table 2. The spacecraft resources required to accommodate each of the instruments are given in Table 3. The allocation for the Solar Wind Ion Composition and Electron Spectrometer includes some allowance for a nadir viewing deflector. The most economical use of these resources is achieved by configurations of instrument into two instrument packages -- Remote Sensing and In-Situ -- each with its own common data processing unit (DPU). With this configuration the total mass and power for the strawman payload is under 20 kg and 20 W respectively. Data rate at the time of closest approach is over 112 kbits/s, roughly half of which will be transmitted in real time, with the rest stored on board for transmission after the perihelion passes.

Solar Probe Spacecraft. The unique feature of the Solar Probe spacecraft is the large but low mass carbon-carbon parabolic heat shield to provide thermal protection for the payload and spacecraft (Fig. 7). This side-mounted heatshield, serving also as the high-gain antenna, has undergone extensive development and testing. In particular, tests of the carbon-carbon material to be used for the heat shield indicate that the mass loss rate is insignificant. Nadir viewing for the visible and XUV imagers is accomplished by means of carbon-carbon tubes that penetrate the heat shield and spacecraft bus. It is recognized that the baseline mission with two perihelion passes requires an Advanced Radioisotope Power Source (ARPS). An ARPS is baselined for each of the other two missions (Europa and Pluto) in the Outer Solar System/Solar Probe Program.

Baseline Mission. Solar Probe is planned to be launched by a Delta III in February 2007 on a direct trajectory to Jupiter to minimize flight time. Gravity assist by Jupiter 1.5 years after launch places Solar Probe in a highly elliptic polar orbit around the Sun. Solar Probe's closest approach at 4 R_S takes place in late 2010, 3.6 years after launch. At perihelion the orbital plane is perpendicular to the Sun-earth line which permits use of the parabolic, side mounted heat shield as the high gain antenna. Because the first encounter is at solar maximum activity, thus precluding observations of the less complicated Sun at solar minimum, a second perihelion pass is now baselined. This will take place in early 2015 at solar minimum. Again, closest approach will be at 4 R_S, with the orbital plane again perpendicular to the Sun-earth line allowing real-time high rate data transmission.

The near perihelion trajectory and activities are shown in Fig. 8. For each of the two passes, encounter measurements by the in-situ instruments start at 10 days before closest approach and end 10 days after perihelion passage. During this twenty day period, the inner heliosphere (< ~0.5 AU) and the corona will be observed in-situ for the first time. Helioseismology observations begin at -4 days (0.2 AU) from closest approach. The most intense observation by all instruments will take place in the two-day period at distances of < 20 R_S from the Sun. During this period Solar Probe will make high time resolution in-situ measurements in the inner corona, high spatial resolution pole to equator to pole observations of the solar surface, and three-dimensional pictures of the solar corona as Solar Probe flies through it.

4. SUMMARY

Solar Probe, one of the first 3 missions in the Outer Solar System/Solar Probe Program of NASA, is scheduled to be launched in February 2007. A highly capable payload of three remote sensing and five in-situ miniaturized instruments will make unprecedented measurements of the inner heliosphere and polar regions of the Sun both at solar maximum and solar minimum. Solar Probe is a mission of exploration, discovery and comprehension, investigating the last uncharted regions of the Sun and solar system. Progress to make substantial improvements in our understanding of solar wind origin and the dynamics of the Sun is not possible without the critical in-situ measurements in the solar wind acceleration region, and the high spatial resolution observations of the polar regions of the Sun.

Acknowledgments. We wish to thank all members of the current and previous Solar Probe Science Definition teams for critical contribution in defining the Solar Probe Mission. The progress made in making this challenging mission technically feasible and ready for development and launch would not have been possible without the support of the talented JPL engineering staff. Portions of the work were performed at the Jet Propulsion Laboratory, Calif. Inst. Tech. under contract with NASA.

REFERENCES

Bruno, R., U. Villante, B. Bavassona, R. Schwenn, and F. Mariani, "In-situ observations of the latitudinal gradients of the solar wind parameters during 1976 and 1977", *Solar Physics*, **104**, 431, 1986.

Geiss, J., G. Gloeckler, R. von Steiger, H. Balsiger, L. A. Fisk, A. B. Galvin, F. M. Ipavich, S. Livi, J. F. McKenzie, K. W. Ogilvie and B. Wilken, "The Southern High Speed Stream: Results from SWICS/Ulysses", *Science*, **268**, 1033-1036, 1995.

Gloeckler, G. and J. Geiss, "Measurement of the abundance of Helium-3 in the Sun and in the Local Interstellar Cloud with SWICS on Ulysses" *Space Science Reviews* **84**, in press, 1998.

Gloeckler, G., L. A. Fisk, S. Hefti, N. Schwadron, T. Zurbuchen, F. M. Ipavich, J. Geiss, P. Bochsler, R. Wimmer, "Unusual composition of the solar wind in the 2 May 1998 CME observed with SWICS on ACE", *Geophys. Res. Lett*, submitted, Aug. 1998.

Habbal, S. R., et al., *Ap. J.*, **489**, L103, 1997.

Kakinuma, T., "Observations of interplanetary scintillation: solar wind velocity measurements", in *Study of traveling interplanetary phenomena*, edited by M. A. Shea et al., D. Reidel Publishing Company, Dordrecht-Holland, 101, 1977.

Kohl, J. L., et al., *Solar Phys.*, **175**, 613, 1997.

Kohl, J. L., et al., *Ap. J. Lett.*, **501**, in press, 1998.

Li, X, S. R. Habbal, J. L. Kohl, G. Noci, *Ap. J. Lett.*, **501**, in press, 1998.

von Steiger, R., J. Geiss, and G. Gloeckler, "Composition of the Solar Wind", in *Cosmic Winds and the Heliosphere*, (eds. J. R. Jokipii, C. P. Sonnett, and M. S. Giampapa), University of Arizona Press, 581-616, 1997.

Woch, J., W. I. Axford, U. Mall, B. Wilken, S. Livi, J. Geiss, G. Gloeckler, and R. J. Forsyth, "SWICS/Ulysses observations: The three-dimensional structure of the heliosphere in the declining/minimum phase of the solar cycle", *Geophys. Res. Lett.* **24**, 2885-2888, 1997.

travel propagate transport move

FIGURE CAPTIONS

Fig. 1. Polar plot of the solar wind speed with heliographic latitude. Solid curve: 1-day averages of the solar wind proton speed derived from data of the SWICS instrument on Ulysses between 1.4 and 5.4 AU (Woch et al., 1997). Dotted curve: Helios observations in the inner (< 1 AU) heliosphere (Bruno et al., 1986). Dashed curve: Solar wind speed deduced from interplanetary scintillations (Kakinuma, 1977). Unshaded regions indicate coronal hole streams, regions shaded red correspond to slow wind from the streamer belt and those shaded orange to regions with periodic variations between the two. It is quite evident that during solar minimum high speed wind fills most of the heliosphere. (From Woch et al., 1997).

Fig. 2. Ionization fractions (filled circles) of Si (left hand panel) and Fe (right hand panel) observed in the high speed solar wind with SWICS/Ulysses. The solid curves are equilibrium freeze-in distributions for temperatures of 1.35 and 1.23 MK, respectively. For iron curves for 1.13 and 1.33 MK (dashed curves) are also shown. The narrowness of the observed charge distributions indicates a single (but different) freeze-in temperature for each element and implies that temperatures at the freeze-in altitudes are homogeneous down to the smallest scale. (From Geiss et al., 1995).

Fig. 3. Abundance of indicated elements relative to Oxygen in the high speed stream (bars) and in the slow solar wind (circles) versus First Ionization Time (FIT). FIT, the average time it takes to ionize a given atom in the chromosphere, is closely related to its First Ionization Potential (FIP). The composition in the fast solar wind resembles most closely the photospheric abundances, indicating that the solar wind from these regions has experienced little compositional changes. (From Geiss et al., 1995).

Fig. 4. Ionization fraction of iron in the slow interstream wind. In contrast to the charge distributions in the fast wind (Fig. 2) the slow wind charge distributions are broad and cannot be modeled using a single freeze-in coronal electron temperature. These observations imply that the slow wind is a mixture of different sources with different freeze-in temperatures.

Fig. 5. Superposed epoch plot of the SWICS/Ulysses data (day 191, 1992 to day 98, 1993) when Ulysses repeatedly crossed the boundary of the high speed stream once every solar rotation (26 days). Shown are the solar wind He speed (dashed curve), the coronal freeze-in temperature of Oxygen, and the Mg/O abundance ratio (solid and shaded curve and filled circles, respectively). The data are repeated for two cycles to reveal the entire pattern. The steep changes in both the freeze-in temperature and abundance ratio demonstrate the existence of a sharp of the high-speed stream reaching into the corona and chromosphere. (Adapted from Geiss et al., 1995).

Fig. 6. Parameters of the initial solar wind inferred from model calculations and remote-sensing 1 AU observation of the coronal hole (left hand panels) and the equatorial region (right hand panel) of the Sun. In the upper left hand panel the speeds of protons (open triangles and squares) and of Oxygen (filled triangles) are based on UVCS/SOHO measurements (Kohl et al, 1997; 1998), as are the effective temperatures for the indicated ions (lower left and right hand panels). The observations, in spite of significant errors, show clearly that the coronal hole is still being accelerated at 4 R_S and is a factor of ~5 lower than its terminal speed of 800 km/s, and that the effective temperature of heavy ions (Mg and O) is far greater than that of protons in both the coronal hole wind as well as in the equatorial wind.

Fig. 7. Side view of a possible Solar Probe spacecraft showing the parabolic side-mounted heatshield/high gain antenna, the two conically shaped secondary heat shields and the spacecraft bus. Instruments are mounted on the sides and inside the bus and on the boom. The size and shape of the bus and the length of the boom are constrained to fit inside the umbra of the heat shield. Nadir viewing for the plasma instrument is achieved by means of an ion deflection system. A possible configuration of a plasma deflector is shown on the left side of the spacecraft.

Fig. 8. The Solar Probe trajectory as seen from Earth at ± 30 days from perihelion. An enlarged view of the critical science acquisition phase for ± 1 day is shown on the right. Two perihelion passes, one at solar maximum and one at solar minimum, are planned for the baseline Solar Probe Mission to be launched in February 2007.

Solar Wind Speed with Heliographic Latitude
SWICS/Ulysses Observations

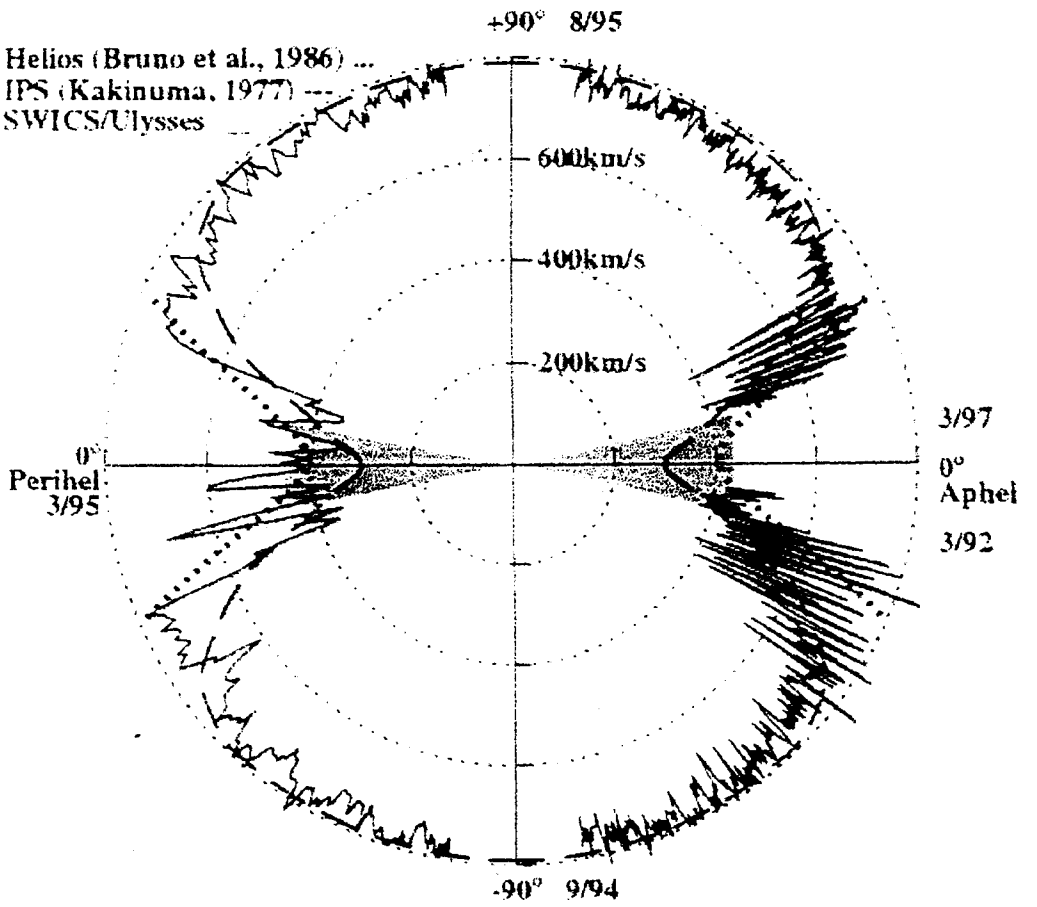

Fig 1

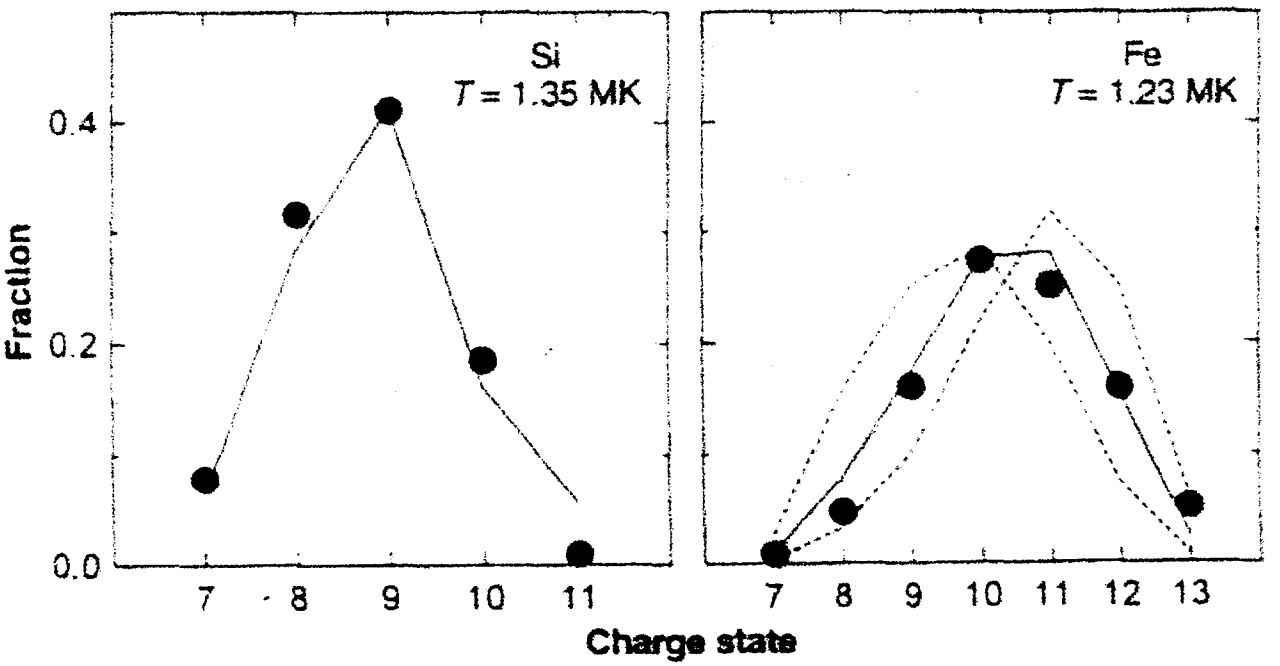
Si
T = 1.35 MK
Fe
T = 1.23 MK
Fraction
0.4
0.2
0.0
7
8
9
10
11
12
13
Charge state

G.G Fig 2

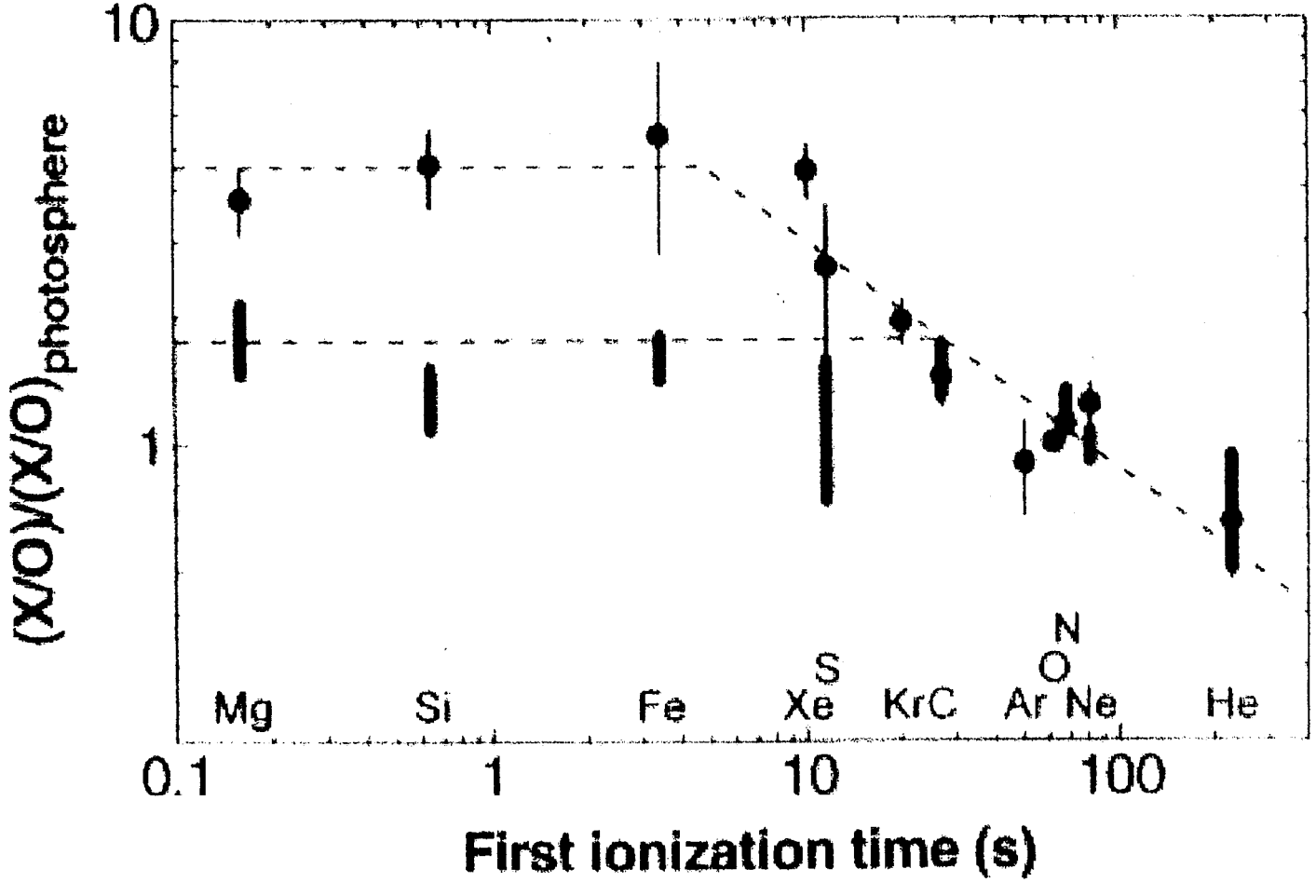
10
1
$(X/O)/(X/O)_{photosphere}$
Mg
Si
Fe
S
Xe
KrC
N
O
Ar
Ne
He
0.1
1
10
100
First ionization time (s)

Fig 3

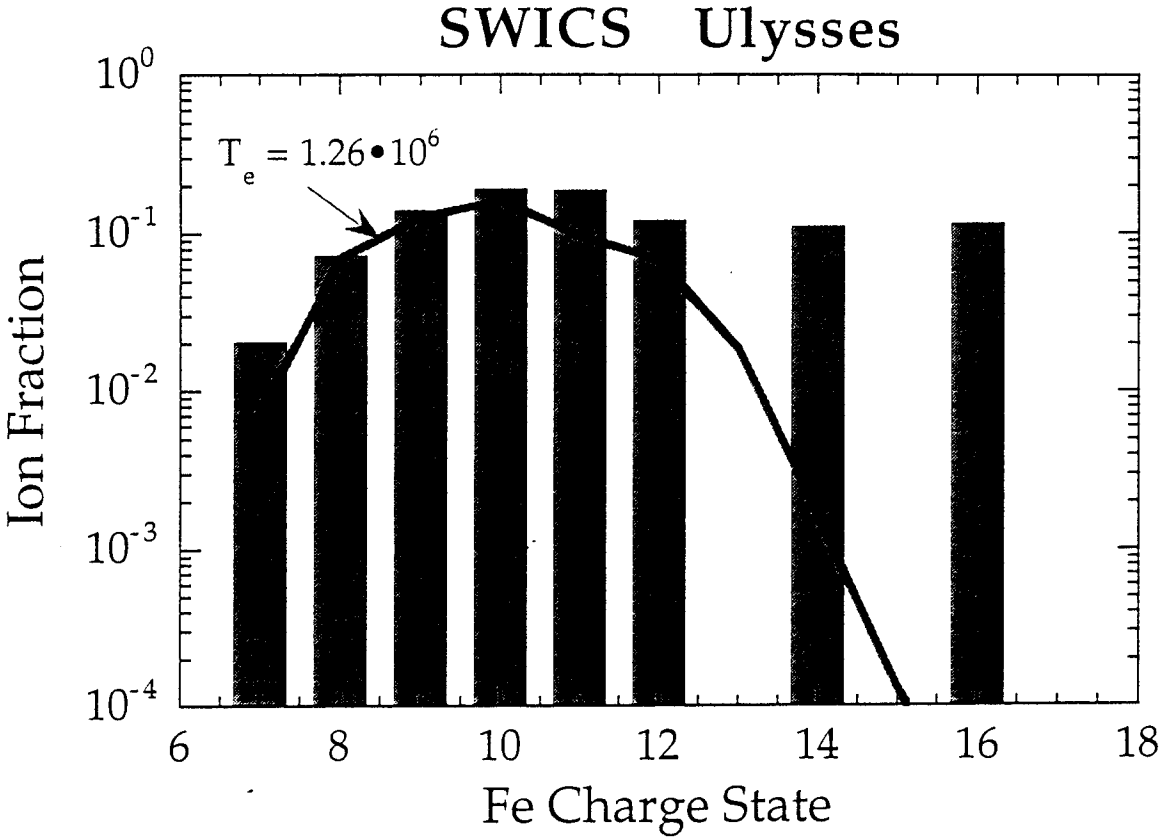
SWICS Ulysses
10^0
10^{-1}
10^{-2}
10^{-3}
10^{-4}
$T_e = 1.26 \bullet 10^6$
Ion Fraction
6
8
10
12
14
16
18
Fe Charge State

G.G Fig 4

Variations in Charge State and Elemental Composition:

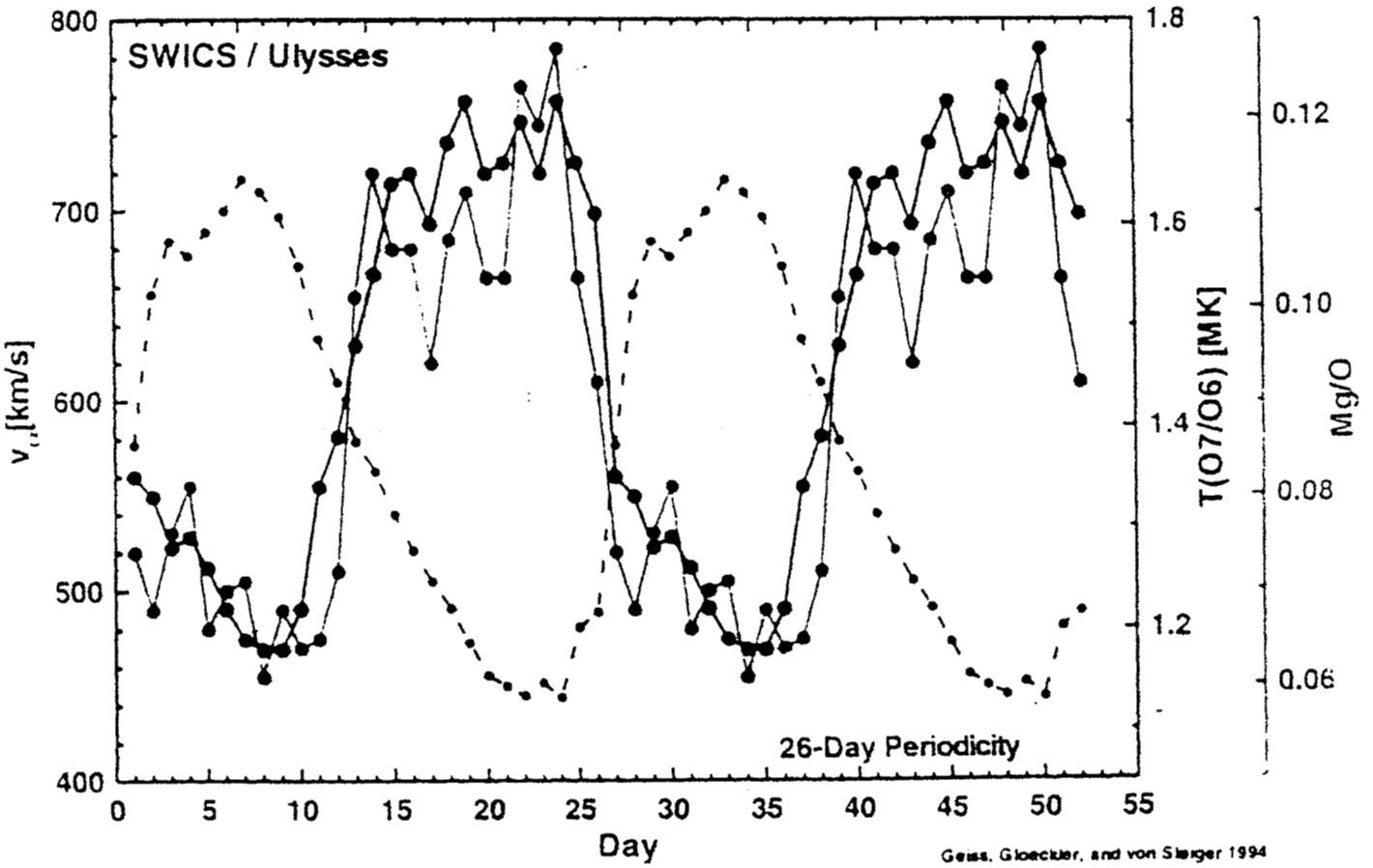

66 Fig 5

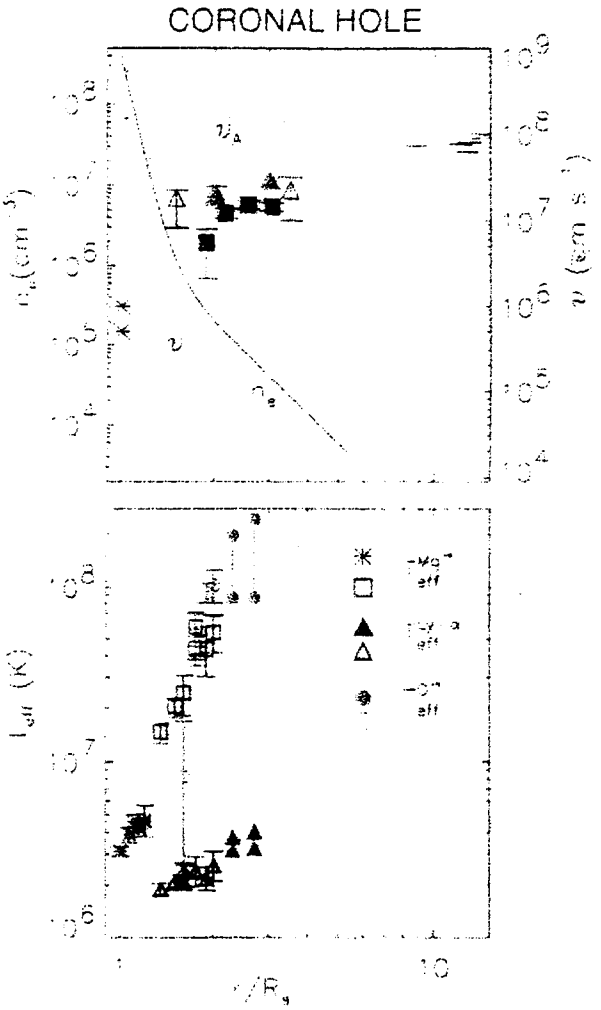
CORONAL HOLE
v_A
v
n_e
n_e (cm^{-3})
v (cm s^{-1})
T_{eff} (K)
r/R_s
10

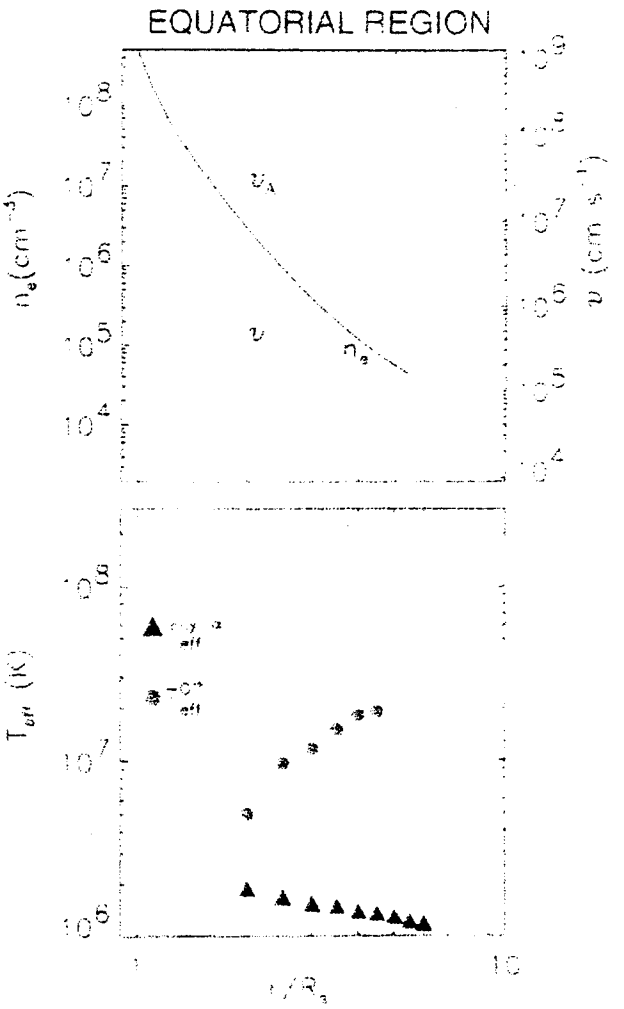
EQUATORIAL REGION
v_A
v
n_e
n_e (cm^{-3})
v (cm s^{-1})
T_{eff} (K)
r/R_s
10

G.G Fig 6

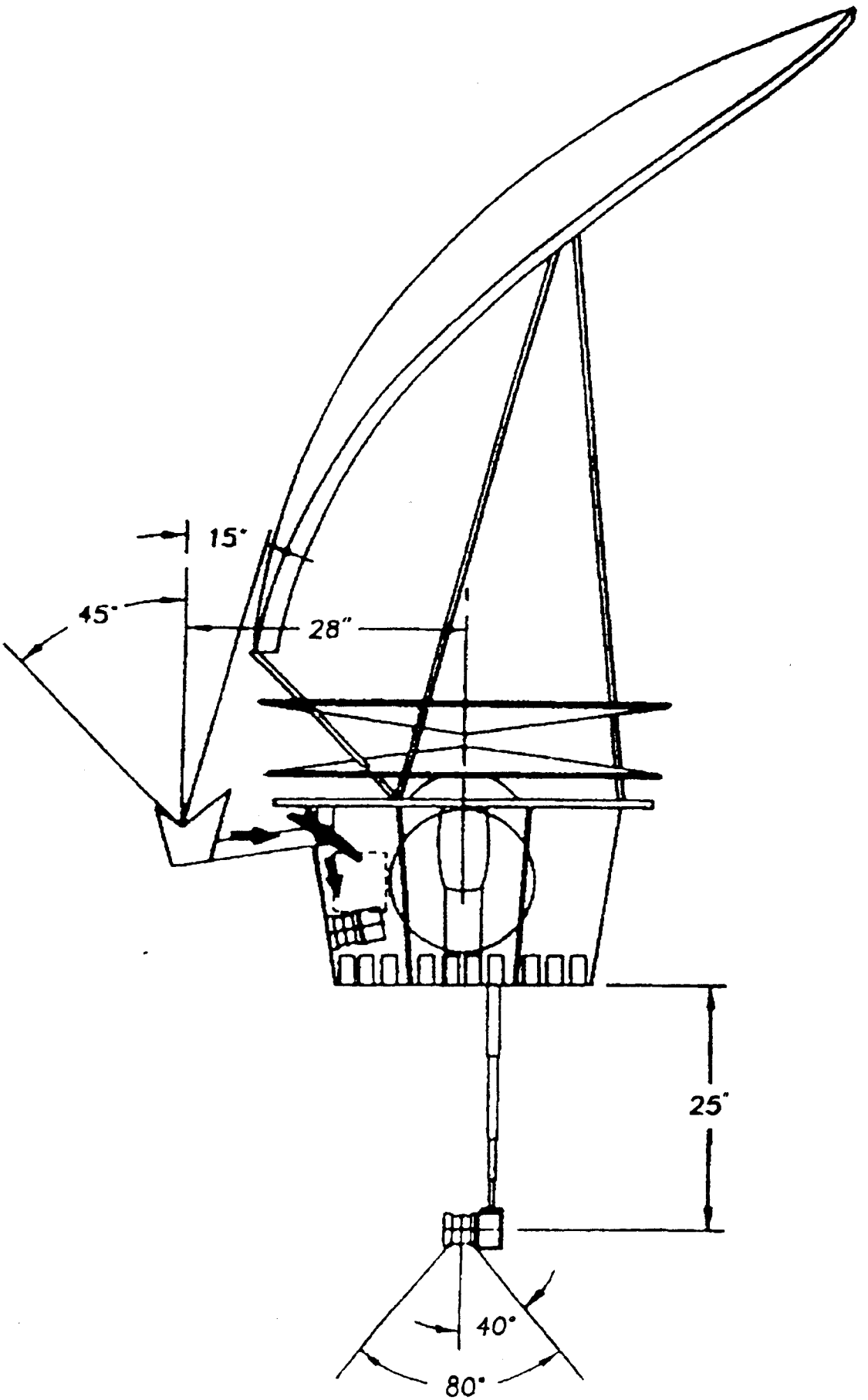

G.G Fig 7

Near Perihelion Activities
(View from Earth)

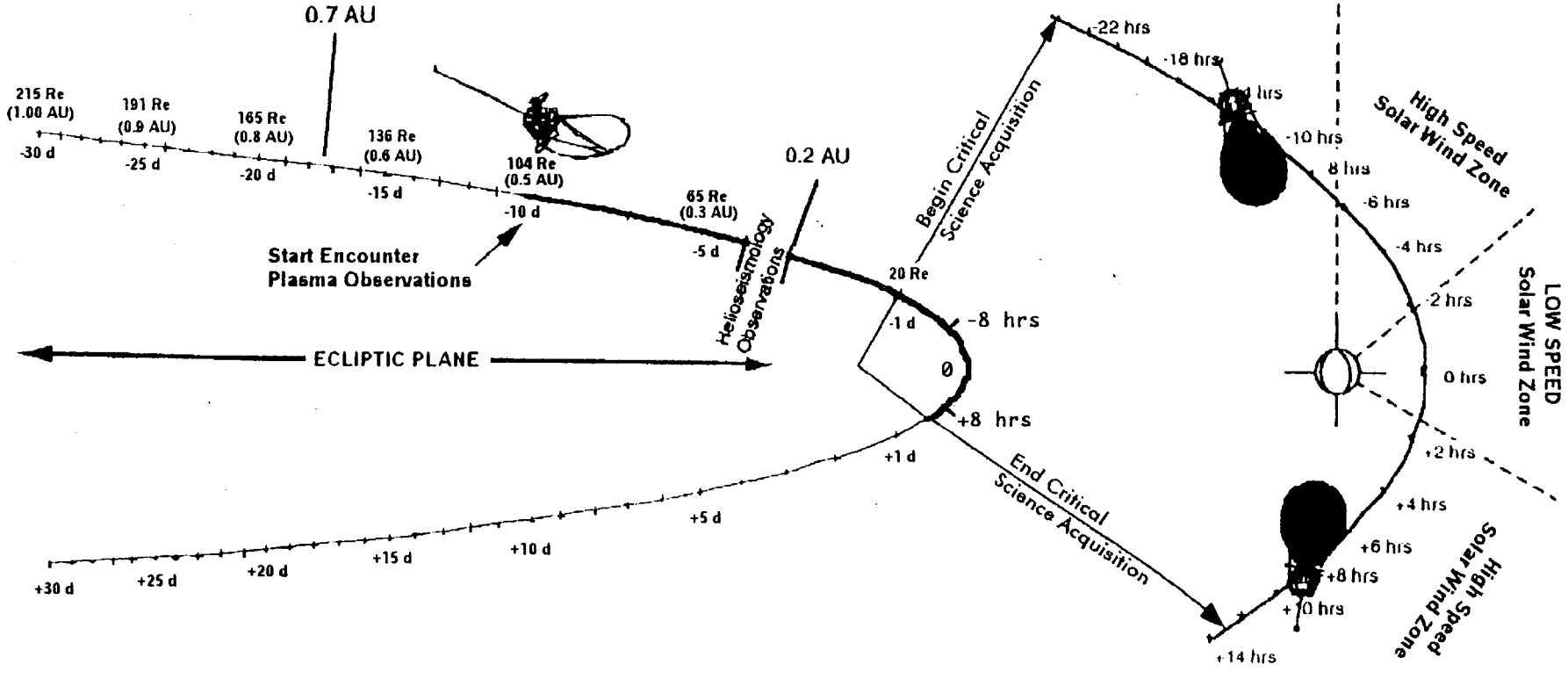

C.C. Fig 8

Table 1. Solar Probe Science Definition Team.

Member	Affiliation
William Feldman	Los Alamos National Labs
George Gloeckler, Chair	University of Maryland
Shadia Habbal	Harvard Smithsonian
Clarence Korendyke	Naval Research Laboratory
Paulett Liewer	Jet Propulsion Laboratory
Ralph McNutt	Johns Hopkins University/APL
Eberhard Möbius	University of New Hampshire
Thomas Moore	Goddard Space Flight Center
James Randolph	Jet Propulsion Laboratory
Robert Rosner	University of Chicago
James Slavin	Goddard Space Flight Center
Bruce Tsurutani	Jet Propulsion Laboratory

Table 2 Solar Probe Strawman Instruments: Measurement Requirements

Strawman Instruments	Parameter(s), or Quantity(ies) Measured	Sensitivity, *Dynamic Range*	Spectral Range, *Resolution*	Angular Range, *Resolution*	Time or Spatial Resolution*
Remote Sensing Instrument Package					
Visible Magnetograph - Helioseismograph	Magnetic Field, Line-of-Sight Velocity Field, Intensity	10 G *10-3000* G 20 m/s *10-4000* m/s 1% *1-400* %	3 Å Visible *70* mÅ	1024 arc sec *2* arc sec	2 sec 32 km
XUV Imager	Intensity @ Entrance aperture	100 ergs/cm^{2}sr *100-40,400* ergs/cm^{2}sr	EUV Band providing Coronal Imaging, *8*Å	2560 arc sec *5* arc sec	< 1 sec
All-sky, 3 - D Coronagraph Imager	White light	Signal to Noise > 100, > *1000*	400-700 nm	20-180° from S/C-Sun line *< 1°*	< 1 min
In-Situ Instrument Package					
Magnetometer	Vector DC Magnetic Field	±0.05 nT *10^3*	---	---	10 ms 3 km
Solar Wind Ion Composition and Electron Spectrometer	Dist. fncs of dominant charge states of H, He, C, O, Ne, Si and Fe; electrons	10^5/cm^{2}s *$2 \cdot 10^7$*	0.05 < E < 50 keV/e *ΔE/E < 0.07*	Nadir and 135° x 300° (2π) *10° x 10°*	1 sec for H, He, e$^-$; 10 sec for heavy ions
Energetic Particle Composition Spectrometer	Differential fluxes of H, ^{3}He, ^{4}He, C, O, Si, Fe, and electrons	10/cm^{2}s-sr keV *10^7*	0.02 < E < 20 MeV/n e$^-$: 0.02 - 1.0	135° x 300° *20° x 20°*	1 sec

Plasma Wave Sensor	AC Electric and Magnetic Fields	10^{-5} V/m 10^{-9} nT/Hz 10^6	MeV $\Delta E/E < 0.07$ 0.05 - 150 kHz $\Delta\omega/\omega = 0.05$	---	1 ms (wave cap) 1 sec (spectral)
Fast Solar Wind Ion Detector	Dist. fcn of ions	$10^6/cm^2s$ 10^6	$0.02 < E < 50$ keV/e $\Delta E/E < 0.07$	90° x 300°	1 ms

Table 3 Solar Probe Strawman Payload: Instrument Requirements

Strawman Instruments	Mass (kg)	Power (W)	Data Rate (kbps)
Remote Sensing Instrument Package			
Visible Magnetograph - Helioseismograph	3.0	1.2	30
XUV Imager	3.0	1.2	30
All-sky, 3 - D Coronagraph Imager	2.8	2.0	2
DPU for Remote Sensing Instruments	0.3	0.8	--
In-Situ Instrument Package			
Magnetometer (with boom cables)	0.8	0.5	1.2
Solar Wind Ion Composition and Electron Spectrometer (with nadir viewing)	4.4	4.4	15.6
Energetic Particle Composition Spectrometer	0.7	0.6	4.8
Plasma Wave Sensor (with boom cables)	2.5	2.5	9.6
Fast Solar Wind Ion Detector	1.0	1.5	19.2
DPU for In-situ Instruments	0.3	0.8	--
TOTAL	18.8		